MASS SPECTROMETRY IMAGING STUDY OF LIPID METABOLITES IN THE ADULT MOUSE TESTIS

Sheba Jarvis[1]; Mark Towers[2]; Paul Murray[2]; Charlotte Bevan[1]; Emmanuelle Claude[2]
[1]Imperial College London, Hammersmith hospital, London, UK; [2]Waters Corporation, Wilmslow, UK

INTRODUCTION

The testis is a complex and heterogeneous organ with endocrine and exocrine functions. Lipid homeostasis is crucial for these functions.
The most abundant testicular lipids, seminolipids, (accounting for 3% of total lipids) are selective to maturing germ cells and crucial for male fertility. These are well described in other literature[1,2].
Furthermore, phosphatidylcholines (PCs) play a major role on the structure and function of testes[3].
A comprehensive understanding of the overall lipid metabolites localisation is critical to understand testicular function and to this day, studies have been limited to specific lipid classes.
With the technical improvement of ionization sources such as matrix-assisted laser/desorption ionization (MALDI) and desorption electrospray ionization (DESI-MSI), it is now possible to achieve pixel sizes that specifically distinguish the complex testicular anatomy.

Here we used a multi-modal mass spectrometry imaging (MSI) approach with MALDI-MSI and DESI-MSI as complementary approaches to improve the characterization of testicular lipid metabolites.

METHODS

Tissue sample preparation

Experiments were conducted on mouse testis tissue sections, which were sectioned using a cryotome, deposited onto standard microscope slides and preserved at -80°C until analysis by mass spectrometry was performed.
For MALDI experiments, a SunCollect nebulizing spray device was used to evenly apply several coatings of α-Cyano-4-hydroxycinnamic acid (CHCA), 5 mg/mL solution in acetonitrile/water (70/30 *v/v*) for positive mode analysis, and 9-aminoacridine (9-AA), 5mg/mL solution in methanol/water, (70/30 *v/v*).

DESI imaging experiments require no sample preparation as desorption and ionization are initiated by charged droplets (98% MeOH, 2% water) impacting directly on the surface.

Mass spectrometry

MALDI MSI experiments were carried out on a MALDI SYNAPT HDMS G2-S*i* mass spectrometer in positive and negative ionisation modes, with a mass range of m/z 100—1,200. The intermediate vacuum MALDI source employed a solid-state diode-pumped Nd:YAG laser with a repetition rate of up to 2.5 KHz .

DESI MSI experiments were carried out on a Xevo G2-XS Q-ToF mass spectrometer in positive and negative ionization modes, with a mass range of m/z 100—1,200

MALDI-MS

Laser:	Nd:YAG laser (355 nm)
Pulse rate:	1000 Hz
Pixel size:	30 µm (lateral)

DESI-MS

Flow rate:	1.5 µl/min
Capillary voltage:	4.5 kV
Nebulising gas:	5 bar
Pixel sizes:	25 and 50 µm (lateral)
Stage speed:	100 µm/s

Data management

Slides were scanned using a flatbed scanner and regions to be imaged were defined in High Definition Imaging Software (HDI) v1.5 (Waters).

DESI and MALDI imaging datasets were mined using MassLynx as well as processed and visualized using HDI 1.5.

Extensive statistical analyses were carried out using EZ Info (Umetrics). Regions of Interest (ROIs) defined in HDI and associated intensities were averaged and TIC normalized in the form of a .csv file which was loaded directly into Metaboanalyst (https://www.metaboanalyst.ca/MetaboAnalyst/faces/home.xhtml).

RESULTS

Lipid difference between cell types in a mouse testis tissue by MALDI imaging in NEGATIVE mode.

Mouse testis was used for the purpose of investigating the different lipid metabolic profiles depending on the various tissue types within the testis, such as the Leydig/blood vessels, mature germ and Sertoli/early germ cell types.

Testis specific lipids have been studied by Ishizuka et al. 1973[4] and identified as sulphated glycerogalactolipid seminolipids.

From the study carried out by Goto-Inoue et al[5], seminolipids were detected in negative mode by MALDI where *m/z* 795.53 (C16:0-alkyl-C16:0-acyl seminolipid) was the most abundant and localized through the tubules, which is in agreement with figure 1.

The other four reported seminolipids were also detected, *m/z* 809.5 (C17:0-alkyl-C16:0-acyl seminolipid), *m/z* 767.5 (C14:0-alkyl-C16:0-acyl seminolipid), *m/z* 821.5 (C18:1-alkyl-C16:0-acyl seminolipid) and *m/z* 823.5 (C18:0-alkyl-C16:0-acyl seminolipid). Other lipids were also detected, mainly phosphatidylinositol (PI), such as PI (38:4) highly localised in the Leydig and blood vessels.

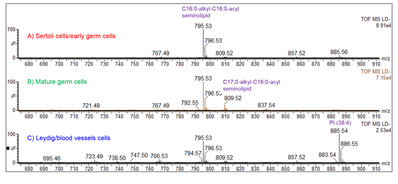

Figure 1: Negative mode MALDI MS spectra from A) Sertoli cells/early ger cells, B) Mature germ cells and C) Leydig/blood vessels cells.

Interestingly, m/z 809 (C17:0-alkyl-C16:0-acyl seminolipid) was localised in the inner lumen of tubules, where spermatid and spermatozoa are presents. It also appears that the abundance of m/z 809 differs from tubules to tubules, probably due to the staging on the tubule.

Figure 2,B displays the results of Principal Component Analysis (PCA) of the ROIs intensity profiles where there is a clear separation between the three groups, demonstrating significant difference in the lipid profiles, figure 2,C shows the loadings plot with the box plots for three lipids m/z 795. 54, m/z 885. 55 and m/z 809.52.

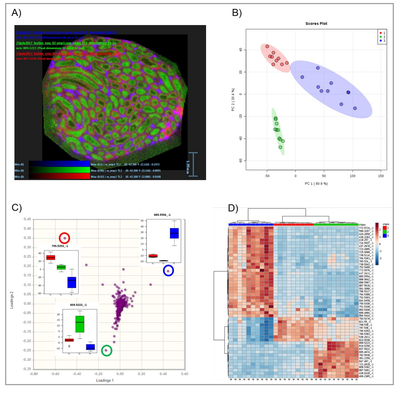

Figure 2: Negative mode MetaboAnalyst statistical analysis A) RBG ion images m/z 857.52, m/z 809.52 and m/z 885.55., B) PCA score plot, C) Loadings plot and D) Heatmap. Red represents Sertoli cells/early germ cells, Green represents mature germ cells and blue represents Leydig/ blood vessel cells.

Regions Of Interest (ROIs) were drawn on the RGB ion image (figure 2,A) specifically to the three cellular regions to compare the MS spectra (figure 1,A,B,C) and the lipid metabolic profiles using statistical tools available in MetaboAnalyst web-based software.

Lipid difference between cell types in a mouse testis tissue by MALDI imaging in POSITIVE mode.

In positive mode, phosphatidylcholines were predominantly detected. These have a key role in the structure and function of testes.

As is shown in figure 3, different cell types have different lipid profiles. The MS spectrum in figure 3,A) shows PC (34:1), PC (34:2) and PC (36:4) were more abundant in the Sertoli cells/germ cell type in a form of H^+, Na^+ and/or K^+. PC (38:5) and PC (38:6) were more abundant in the mature germ cells (figure 3,B), and PC (36:1), PC (36:2), PC 38:4) were highly abundant in the Leydig/blood vessel cells (figure 3,C).

Species in the mass range of m/z 650-750 were identified to be the PCs with a loss of *m/z* 59 or *m/z* 183, respectively being the trimethylamine [$(CH_3)_3N$] and the PC head group [$(CH_2)_2PO_3H$]. This loss could occur within the source region of the mass spectrometer, due to the ionization mechanism.

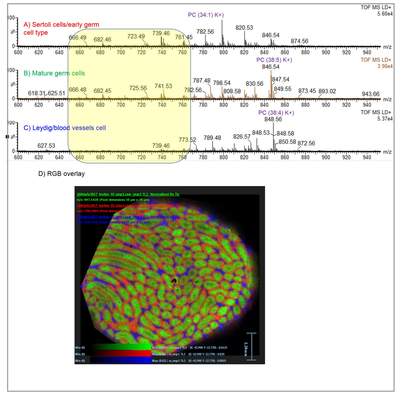

Figure 3: Positive mode MALDI MS spectra from A) Sertoli cells/early ger cells, B) Mature germ cells and C) Leydig/blood vessels cells. D) RBG ion images m/z 798.54, m/z 847.54 and m/z 810.6.

Seminiferous tubules within a single testis section could be at different stage of maturation, containing different cell types, such as spermatogonia (Sg) and nurse cells (Nc) with a few spermatocytes (Sc) in the lumen (early development); spermatids (St) and immature spermatozoa (Sz) within the lumen (mid development); and fully mature Sz and Nc close to the basement membrane (mature development).

It has been reported that different PCs will be specific to the cell types[3] and therefore indicate the stage of maturation of each tubules.

Figure 4 shows the overlay of m/z 820. 5 (PC(36:4), K+) in red and m/z 844.5 (PC(38:5), K+) in green. It can be observed that tubules A are showing intensity mainly from m/z 844.5, whereas both lipids were detected in tubules B.

Similarly, in negative mode, it can be observed from figure 5,A) displaying the RGB overlay ion image that the tubules have different colour, indicating different expressions of *m/z* 809.5 (C17:0-alkyl-C16:0-acyl seminolipid), *m/z* 837.55 (PI(34:0)) and *m/z* 881.52 (PI(38:6) in the different tubules presents in the testis section.

A staging of the tubules from a pathologist is needed, in that case, to correlate the different lipids profiles to the maturation of the tubule.

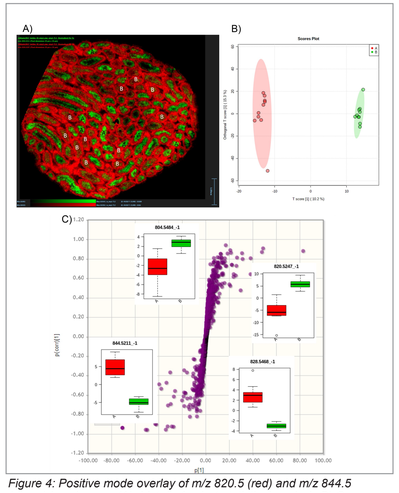

Figure 4: Positive mode overlay of m/z 820.5 (red) and m/z 844.5 (green) ions images (A). MetaboAnalyst statistical analysis B) OrthoPLSDA score plot, C) Loadings plot.

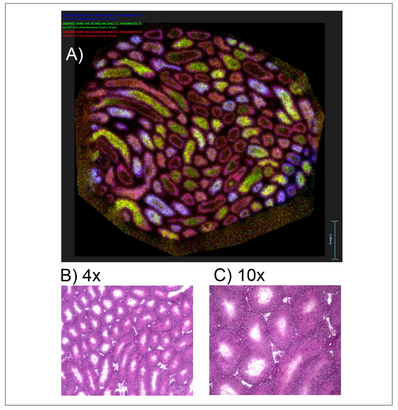

Figure 5: A) Negative mode overlay of m/z 809.52 (C17:0-alkyl-C16:0-acyl seminolipid)(red) and m/z 837.55 (PI(34:0) green) and m/z 881.5 ions image. B) 4x H&E image, C) 10x H&E image.

Comparison between MALDI and DESI in positive mode

Further experiments using a DESI source were carried out at 25 and 50 µm pixel size.
Figure 6 A) shows that lipids above m/z 900 were detected with the testis tissue by DESI but not by MALDI and have been tentatively identified at triglycerides.
Finally, an example in figure 7 shows RGB overlay ion images from DESI imaging experiments run at 25 and 50 µm. At a smaller pixel size, the definition of the features within the testis is more defined than at 50

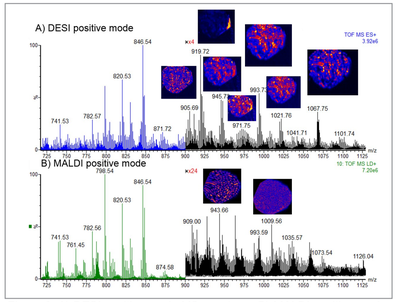

Figure 6: A) DESI positive mode MS spectrum, B) MALDI positive mode MS spectrum; with ion images of lipids m/z above 900

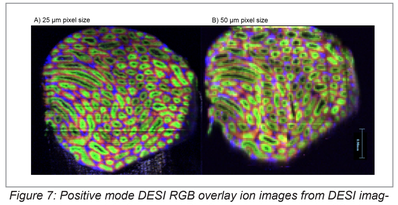

Figure 7: Positive mode DESI RGB overlay ion images from DESI imaging experiments at A) 25 µm and B) 50 µm pixel sizes (m/z 798.54, m/z 847.54 and m/z 810.6).

CONCLUSION

- **Lipid profiles in the different tissue types within a mouse testis are radically different, in both positive and negative mode.**
- **In negative mode, seminolipids were the main peaks detected as well as phosphatidylinositol (PI) such as PI (38:4) highly localised in the Leydig and blood vessels.**
- **In positive mode, mainly phosphatidylcholines were detected in both MALDI and DESI experiments. However triglycerides were mainly detected by DESI.**
- **Within one section, different staging of the tubules can be assessed based on lipid profile.**
- **The DESI imaging experiment at 25 µm gave a sharper image quality than 50 µm.**

References
1. Rodemer C; et al. Human Molecular Genetics; 12: 1881-1885
2. Vos JP; et al. Biochim, Biophys Acta 1211:1250149
3. Siangcham T; et al. PLoS ONE 10(3): e0120412. doi: 10.1371/journal. Pone.0120412
4. Ishizuka I; et al. J Biochem. 1973 Jan; 73(1): 77-87
5. Goto-Inoue, N ; et al. Glycobiology (2009), vol. 19 no. 9 pp. 950-957

TO DOWNLOAD A COPY OF THIS POSTER, VISIT WWW.WATERS.COM/POSTERS